A Two-Dimensional Model for Simulation, Control, and Optimization of FCC Risers

J. A. Souza
Departamento de Física, Universidade Federal do Rio Grande. Av. Itália, Km 08 S/N, Campus Carreiros,
Rio Grande–RS, Brazil

J. V. C. Vargas
Departamento de Engenharia Mecānica, Universidade Federal do Paraná. CP 19011, Curitiba-PR, Brazil

O. F. Von Meien
DUN-RIO/ST/EISA –PETROBRÁS. Av. Gen. Canabarro 500 - 5° andar, Maracanã - Rio de Janeiro-RJ, Brazil

W. Martignoni
Petrobrás S.A. –AB-RE/TR/OT. Av. Chile 65, Sala 2102 –Centro - Rio de Janeiro-RJ, Brazil

S. C. Amico
Departamento de Materiais, Universidade Federal do Rio Grande do Sul. Av. Bento Gonçalves, 9500, Bairro Agronomia,
Porto Alegre–RS, Brazil

DOI 10.1002/aic.10798

A simplified two-dimensional (2-D) formulation for FCC risers has been developed. The model approximates the mixture of gasoil, steam, and solid catalyst that flows inside the riser reactor by an equivalent fluid with average properties. The cracking reactions are modeled by a 6-lump kinetic model combined with two energy equations (gas and solid). Due to the adopted simplifications, a fast and simple-to-solve computational code was written; nevertheless, it still is sufficiently precise to be used for the design of new units and for system control and optimization of operating conditions of FCC risers. The validation of the proposed model was performed by direct comparison of the obtained results with available experimental data for a multi-purpose pilot FCC riser unit. The model was then utilized to simulate an actual size industrial FCC riser. The obtained numerical results in this article demonstrate that the model can be used as a powerful and simple tool for design, control, and optimization of FCC units, combining accuracy with low computational time to obtain solutions when simulating actual FCC riser operation.
AIChE J, 52: 1895–1905, 2006
Keywords: FCC riser, fluid flow and kinetic modeling, numerical simulation

Introduction

The numerical modeling of the FCC (Fluidized Catalytic Cracking) process of a petroleum refinery has been performed by several authors who have proposed different mathematical models and reported them in the open literature.[1-3] With the constant increase of computational capabilities, such models have become even more complex and with wider application. The different models address both fluid flow and cracking kinetic, varying from simple one-phase and one-dimensional (1-D) models to 3-D and three-phase models. Therefore, there is no common ground re-

---

Correspondence concerning this article should be addressed to J. V. C. Vargas at jvargas@demec.ufpr.br.

garding the most adequate formulation for FCC risers modeling, and advantages and drawbacks may be identified in each available model.[4]

In general terms, the fluid flow models for riser reactors may be classified in three categories: (i) 1-D models, normally with simplified formulation and solution[5,6]; (ii) semi-empirical models, usually described as core-annulus models[7-9]; and (iii) models based on phenomenological concepts, more detailed than the other models. These latter models use a simultaneous solution of the conservation equations of mass, momentum, energy, and species for both gas and particulate phases.[2,10]

Another possible way of classifying the different models is based on their direct industrial application. Thus, an FCC riser model (fluid flow and/or kinetic) can be used for: (i) the development of a major model where the simulations of the entire conversion FCC unit is considered; (ii) testing or studying of specific catalytic cracking phenomena, such as catalyst deactivation, adsorption, kinetic models, and so on; (iii) the search for better operating conditions (unit optimization); and (iv) phenomenological studies of the physical problem. For the first type, the models simulate not only the riser, but also other equipment, like the regenerator and the stripper. It is very important to have a fast solution for the riser model, and also to be able to determine coke formation during the cracking reactions as a separate lump. This information will be later used by the regenerator model to determine the energy produced from coke burning and also the temperature of the regenerated catalyst. For this reason, the selected kinetic model must be able of independently determining coke concentration. Han and Chung[3] used a 1-D two-phase fluid flow model, combined with a 4-lump kinetic cracking model, to simulate the entire FCC unit. This kind of model is normally used in the development of control systems, where the most desired feature of the model is a low computational time solution. In these applications, it is not necessary to have an exact determination of the values of the variables (mass concentration and temperatures along the riser), but only to determine qualitatively correct system response to changes in the operating conditions, so that the best action may be taken by the control system.[5,11]

The second type encompasses models used when the main goal is to study a specific physical phenomenon of the gasoil catalytic cracking, such as analysis of a catalyst deactivation function,[12] the coke formation in the cracking process,[13] the adsorption phenomena in the catalytic cracking,[6] and the building of kinetic models.[14] In these cases, it is preferable to have a simple and easy-to-solve mathematical formulation for the fluid flow (normally a plug-flow), allowing concentration on the analysis effort on the phenomenon of interest. Semi-empirical models can also be included in this category and are normally used to describe or study specific characteristics of the complex flow that occurs inside the riser reactor. Examples may be found in Patience et al.,[7] who proposed an empirical correlation to the slip factor, and in Derouin et al.,[8] who presented empirical correlations for the gas and catalyst velocity profiles and the slip velocity between gas and catalyst.

The third type of models strives for unit optimization. In this case, it is necessary to have a fast and sufficiently precise model that will be used to run several simulations (each one for a specific operating condition), searching for the best values for the input variables (mass concentrations, temperatures, and so on). This is a difficult balance (that is, a fast and sufficiently precise model). However, according to Theologos and Markatos,[1] the overall performance of the riser can be predicted by a one-dimensional mass, energy, and chemical species balance, which suggests that simplified models, as in Han et al.[15] and Souza,[16] may be precise enough to be used in an optimization process.

The fourth type refers to models that include all important physical phenomena. These models are generally 3-D with two-phase flow (some models are also three-phase flow). The conservation equations are written for each phase of the fluid flow (gas, solid (catalyst), and liquid droplets) and the physical properties are not necessarily assumed constant, being sometimes added to the model as additional equations. Turbulent models are normally used to describe the fluid flow and, in some formulations, kinetic theory is used to determine the physical characteristics of the particle flow. These models are more suitable for theoretical studies of the physics of the multi-phase flow phenomena that occur inside the riser reactor. They are also used to compare the mathematical models with the experimental data, providing a more comprehensive understanding of the physical phenomena.[2,10]

In addition, the kinetic model is highly responsible for an adequate determination of the mass concentrations of each mixture component along the riser reactor. It is well known that the formulation of a kinetic model that includes all chemical reactions responsible for the catalytic cracking of the gasoil is still not possible. However, it is possible to group the hydrocarbon chains of similar chemical functions into lumps and then make the kinetic model based on a few components (lumps). Again, based on their industrial application, the models may be classified into: (i) those that determine the most important commercial products (usually 4-6 lumps), such as gasoline, LPG, and light cycle oil, and, depending on the particular case, coke[14,17]; and (ii) those that may be used for the phenomenological study of the catalytic cracking reaction, usually with 10 or more lumps.[18,19]

In such a complex scenario, this work addresses the development of a simplified model with a 2-D fluid flow field combined with a 6-lump kinetic model to simulate the gasoil catalytic cracking process inside the riser reactor. Two energy equations (catalyst and gasoil) are utilized to evaluate the temperature gradient between the two phases considered, that is, the catalyst (solid) and the mixture gasoil/lift water vapor (gas).

Mathematical Model

Figure 1 shows the studied system, with its simple geometry, where H is the length of the riser in the flow direction and R is the radius of the riser. Regenerated catalyst, gasoil, and steam enter the system from the bottom of the riser; whereas the product lumps, the deactivated catalyst, and steam leave it from the top of the riser.

In an industrial FCC unit, the catalyst and the lift steam are injected at the bottom of the riser reactor, whereas the gasoil and the atomization steam enter the riser by injection nozzles at a higher radial section. One of the propositions of the present model is to assume the mixture of catalyst, gasoil, and steam is introduced as a single mixture at the bottom of the riser.

The present model also considers the following assumptions: incompressible, laminar, and 2-D flow (cylindrical coordi-

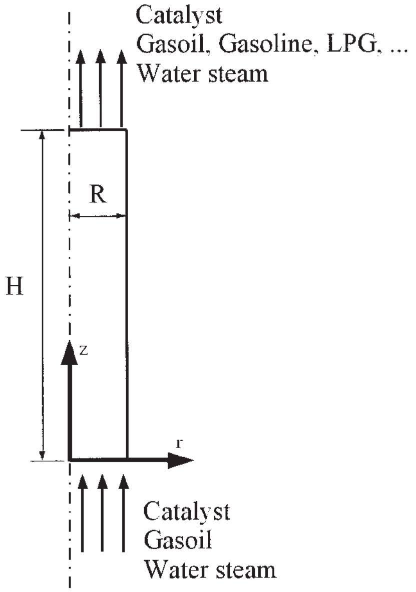

Figure 1. Modeled system.

H: total riser height; R: radius of the riser.

nates), homogeneous mixture (no relative motion between the gas and the particles), and uniform physical properties for the mixture, with the gasoil entering the riser already vaporized.

Therefore, the simplified mass and momentum conservation equations are given by:

$$\frac{\partial v_r}{\partial r} + \frac{v_r}{r} + \frac{\partial v_z}{\partial z} = 0 \tag{1}$$

$$\rho\left(\frac{\partial v_r}{\partial t} + v_r\frac{\partial v_r}{\partial r} + v_z\frac{\partial v_r}{\partial z}\right) = -\frac{\partial p}{\partial r} + \mu\left(\frac{\partial^2 v_r}{\partial r^2} + \frac{1}{r}\frac{\partial v_r}{\partial_r} - \frac{v_r}{r^2} + \frac{\partial^2 v_r}{\partial z^2}\right) \tag{2}$$

$$\rho\left(\frac{\partial v_z}{\partial t} + v_r\frac{\partial v_z}{\partial r} + v_z\frac{\partial v_z}{\partial z}\right) = -\frac{\partial p}{\partial z} + \mu\left(\frac{\partial^2 v_z}{\partial r^2} + \frac{1}{r}\frac{\partial v_z}{\partial r} + \frac{\partial^2 v_z}{\partial z^2}\right) \tag{3}$$

The mixture average density (ρ), in Eqs. 2 and 3, is considered a function of the volumetric fraction of catalyst, gasoil, and steam according to the input conditions of the riser (pressure and temperature). Thus, the average and constant mixture density is calculated for the given riser input conditions by:

$$\rho = \varphi^{\text{in}}_{v\text{go}}\rho_{v\text{go}} + \varphi_{\text{st}}\rho_{\text{st}} + \varphi_{\text{cat}}\rho_{\text{cat}} \tag{4}$$

where the volumetric fractions are given by:

$$\varphi^{\text{in}}_{v\text{go}} = \frac{\forall^{\text{in}}_{v\text{go}}}{\forall}, \quad \varphi_{\text{st}} = \frac{\forall_{\text{st}}}{\forall}, \text{ and } \varphi_{\text{cat}} = \frac{\forall_{\text{cat}}}{\forall} \tag{5}$$

and

$$\forall^{\text{in}}_{v\text{go}} = \frac{\dot{m}^{\text{in}}_{v\text{go}}}{\rho_{v\text{go}}}, \quad \forall_{\text{st}} = \frac{\dot{m}_{\text{st}}}{\rho_{\text{st}}}, \quad \forall_{\text{cat}} = \frac{\dot{m}_{\text{cat}}}{\rho_{\text{cat}}}, \text{ and}$$

$$\forall = \forall^{\text{in}}_{v\text{go}} + \forall_{\text{st}} + \forall_{\text{cat}} \tag{6}$$

where $\forall$ is the volumetric flow rate and $\dot{m}$ the mass flow rate at the riser cross section.

The same approximation was considered for the mixture average viscosity (μ):

$$\mu = \varepsilon\mu_{\text{gas}} + (1-\varepsilon)\mu_{\text{cat}} \tag{7}$$

where ε is the bed porosity.

In Eq. 7, the gas viscosity (μ_{gas}), which was assumed as a weighted average between the viscosities of the gasoil and the steam at the given input conditions, is an input data of the model. For the determination of the catalyst viscosity (μ_{cat}), the expression proposed by Miller and Gidaspow,[20] which was adopted in the current model, calculates the particulate phase viscosity as a function of the catalyst volume fraction (φ_{cat}) as follows:

$$\mu_{\text{cat}} = -0.188 + 537.42\varphi_{\text{cat}} \tag{8}$$

The kinetic model that will determine the conversion rates of the products during the cracking process was based on 6 lumps, as shown in Figure 2.[17] In this model, the primary reactions are of second order, while all other reactions are of first order. The matrix layout of the 15 pre-exponential kinetic constants used to describe the gasoil catalytic cracking is shown below:

$$\begin{bmatrix} 0 & K_{12} & K_{13} & K_{14} & K_{15} & K_{16} \\ 0 & 0 & K_{23} & K_{24} & K_{25} & K_{26} \\ 0 & 0 & 0 & K_{34} & K_{35} & K_{36} \\ 0 & 0 & 0 & 0 & K_{45} & K_{46} \\ 0 & 0 & 0 & 0 & 0 & K_{56} \\ 0 & 0 & 0 & 0 & 0 & 0 \end{bmatrix} \tag{9}$$

The dependence of the kinetic constants on temperature and activation energy is obtained from the matrix presented in Eq. 9 and the Arrhenius Law, where the reaction constants (K^r_{ij}) are given by:

$$K^r_{ij} = K_{ij}e^{(-E_{ij}/\bar{R}T_{cat})} \quad (i, j = 1, 6) \tag{10}$$

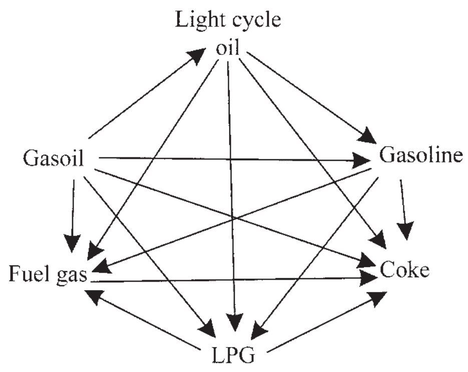

Figure 2. Lumped kinetic model.

The volumetric rate of creation or consumption of species "i" in the cracking reactions is calculated by ref. [6]:

$$\Omega_i = \left[\sum_{j=1}^{i-1} M_j K^r_{ji} (C^r_j)^{n_j} - \sum_{j=i+1}^{N} M_i K^r_{ij} (C^r_i)^{n_i} \right] \phi(1-\varepsilon) \frac{\rho_{\text{cat}}}{M_i} \tag{11}$$

where:

$$C^r_i = \frac{1-\varepsilon}{\varepsilon} \rho_{\text{cat}} K^r_{\text{ad,i}} C_i \tag{12}$$

Adsorption, the physical phenomenon of molecules depositing onto the catalyst and its pore surface, is also important for petroleum catalytic cracking modeling[6] and should preferably be included in the kinetic model. In the present formulation, its influence is incorporated into the model by the adsorption constants $K_{\text{ad,i}}$. The dependence of the adsorption constant on temperature is correlated by the Arrhenius Law as follows:

$$K^r_{ad,i} = K_{ad,i} e^{(-E_{ad,i}/\bar{R}T_{cat})} \tag{13}$$

where $E_{\text{ad,i}}$ is the adsorption activation energy (kJ/kmol) and i is the number of the correspondent lump.

Catalyst deactivation, another important phenomenon, was included in the kinetic model as a simple exponential function given by:

$$\phi = e^{(-406.4 C_c)} \tag{14}$$

where C_c is the coke content of the catalyst ($\text{kg}_c/\text{kg}_{\text{cat}}$).

Combination of Eqs. 10-14 allows the writing of a transport equation for each lump of the kinetic model:

$$\frac{\partial C_i}{\partial t} + v_r \frac{\partial C_i}{\partial r} + v_z \frac{\partial C_i}{\partial z} = \Omega_i \tag{15}$$

where i varies from 1 to the total number of lumps (N). In the present model, based on Figure 2, with N = 6, the lumps are organized as i = 1: vgo; i = 2: light cycle oil; i = 3: gasoline; i = 4: LPG; i = 5: fuel gas; and i = 6: coke.

Diffusive terms were not included in Eq. 15 since a one-phase is considered (no diffusion between the phases). This is also due to the high velocity of the flow inside the riser, which makes the diffusive terms negligible in comparison with the advective ones in the species conservation equations.

Furthermore, even though a one-phase model was adopted in the fluid flow formulation, it was necessary to characterize the temperature gradient between gas and particulate phases. In the reaction (source) term of Eq. 15 (Ω_i, given by Eq. 11), the catalyst temperature is used to calculate the reaction kinetic constants, while for the heat exchange between the particulate and gaseous phases, a second energy equation is necessary. Here, the diffusive terms are also negligible in comparison with the advective ones due to high flow velocities. Thus, the two energy equations, the particulate (catalyst) and the gas (gasoil + steam), were written as follows:

$$\varphi_{\text{cat}} \rho_{\text{cat}} Cp_{\text{cat}} \left(\frac{\partial T_{\text{cat}}}{\partial t} + v_r \frac{\partial T_{\text{cat}}}{\partial r} + v_z \frac{\partial T_{\text{cat}}}{\partial z} \right) = h_{\text{gs}}(T_{\text{cat}} - T_{\text{gas}}) + [(\Delta h_{vgo}) \Omega_{vgo} M_{vgo} + (\Delta h_{\text{coke}}) \Omega_{\text{coke}} M_{\text{coke}}] \tag{16}$$

and

$$(\varphi^{\text{in}}_{vgo} \rho_{vgo} Cp_{vgo} + \varphi_{\text{st}} \rho_{\text{st}} Cp_{\text{st}}) \left(\frac{\partial T_{\text{gas}}}{\partial t} + v_r \frac{\partial T_{\text{gas}}}{\partial r} + v_z \frac{\partial T_{\text{gas}}}{\partial z} \right) + h_{\text{gs}}(T_{\text{cat}} - T_{\text{gas}}) = 0 \tag{17}$$

The water vapor was not considered as a component in Eq. 15 since it does not participate in the reactions' kinetic scheme. However, its influence on the thermal balance is important and for this reason it is considered in the gas energy equation.

Numerical Solution

The mathematical model presented in the previous section was developed for the transient regime for completeness of the introduced formulation. However, in this study, only steady state solutions were obtained, although the model and code developed have the potential for conducting a fully transient analysis for control and optimization purposes.

In the present formulation, the incorporation of the discussed simplifications into the mathematical model has allowed for a fast numerical solution. The finite differences method was used to obtain the steady state solution of the set of partial differential equations of the mathematical model, after dropping the time derivatives, over the geometry shown in Figure 1, with boundary conditions specified as shown in Figure 3. The resulting non-linear system of algebraic equations was solved with the Newton-Raphson method.

For the fluid flow problem (Eqs. 1-3), pressure and input velocities need to be specified at the riser input section. The input pressure is a known operating condition of the unit, while the input velocity (V_{in}) can be calculated by the known mass flow rates, average mixture density (ρ), and riser cross sectional area (A) as follows:

$$V_{\text{in}} = \frac{\dot{m}_{\text{cat}} + \dot{m}^{\text{in}}_{vgo} + \dot{m}_{\text{st}}}{\rho \text{A}} \tag{18}$$

For the transport equation of the kinetic model (Eq. 15), at the input section of the riser, it is considered that only gasoil is entering. Therefore, the mass fraction of gasoil is set to 1, while the other kinetic lumps' mass fractions are set to zero. Then, the concentration of gasoil at the input section of the riser is given by:

$$C^{\text{in}}_{vgo} = \frac{\dot{m}^{\text{in}}_{vgo}}{\dot{m}_{\text{total}}} \frac{\rho}{M_{vgo}} \quad (\dot{m}_{\text{total}} = \dot{m}_{\text{cat}} + \dot{m}^{\text{in}}_{vgo} + \dot{m}_{\text{st}}) \tag{19}$$

At the riser output section, it was considered that the lumps' concentrations are no longer varying, and the derivative in the flow direction is set to zero, for each lump concentration (C_i). This condition is actually true only if the riser is long enough, such that all cracking reactions have already ceased at the top of the riser. If the riser is not sufficiently long, this boundary

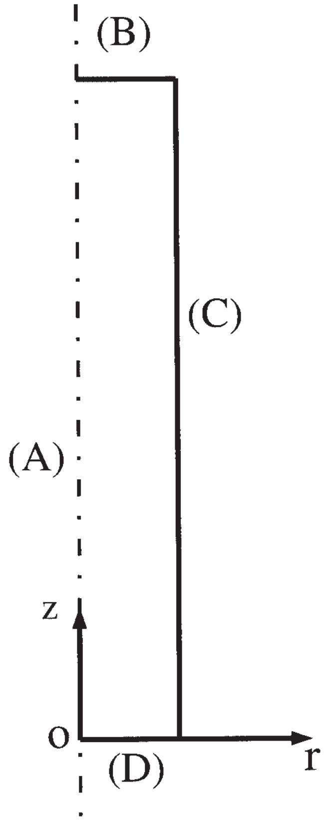

Figure 3. Boundary conditions and computational domain.

condition will flatten the concentration curves near the riser output section, which could induce errors in the lump concentration curves along the riser. In all simulations performed in this work, the riser height was set at least 40 times larger than its diameter, such that the reactions were assumed to have ceased before the riser output section.

To close the energy balance, it is necessary to make another important consideration. In the present formulation, the gasoil enters the riser completely vaporized; therefore, it is necessary to make a correction in the temperature of the catalyst that comes from the regenerator. In the present model, the vaporization of the gasoil is assumed to occur right at the moment of contact with the hot catalyst that comes from the regenerator. So, the gasoil evaporation enthalpy must be accounted for in the global energy balance. This is done by simply correcting the temperature of the catalyst that comes from the regenerator. Recall that all the energy needed by the cracking process and the vaporization of the gasoil comes from the hot catalyst; therefore, an energy balance is written to account for the gasoil evaporation enthalpy as follows:

$$\dot{m}_{\mathrm{cat}} Cp_{\mathrm{cat}}(T_{\mathrm{cat}}^{\mathrm{in}} - T_{\mathrm{cat}}^{\mathrm{in,c}}) = \dot{m}_{vgo}^{\mathrm{in}} h_{\mathrm{fg},vgo}(T_{vgo}^{\mathrm{in}}) \tag{20}$$

where $h_{\mathrm{fg},v\mathrm{go}}(T_{v\mathrm{go}}^{\mathrm{in}})$ is the gasoil evaporation enthalpy at $T_{v\mathrm{go}}^{\mathrm{in}}$, $T_{\mathrm{cat}}^{\mathrm{in}}$ is the temperature of the catalyst that comes from the regenerator, and $T_{\mathrm{cat}}^{\mathrm{in,c}}$ is the corrected input catalyst temperature.

Rearranging Eq. 20, the corrected input catalyst temperature at the riser input is calculated by

$$T_{\mathrm{cat}}^{\mathrm{in,c}} = T_{\mathrm{cat}}^{\mathrm{in}} - \frac{\dot{m}_{v\mathrm{go}}^{\mathrm{in}} h_{\mathrm{fg},v\mathrm{go}}(T_{v\mathrm{go}}^{\mathrm{in}})}{\dot{m}_{\mathrm{cat}} Cp_{\mathrm{cat}}} \tag{21}$$

For the energy equations (Eqs. 16 and 17), the riser walls are considered adiabatic; therefore, the zero energy flux boundary condition is set at the walls of the riser for both gas and catalyst phases. The same boundary conditions are prescribed at the central axis of the riser due to symmetry. Finally, at the top of the riser, temperatures for both gas and catalyst phases are also no longer varying, and the temperature derivatives in the flow direction are set to zero.

Figure 3 shows the computational domain and the appropriate boundary conditions for the problem, as follows:

$$(\mathrm{A}) \begin{cases} v_r = 0, \quad \dfrac{\partial v_z}{\partial r} = 0 \\ \dfrac{\partial T_{\mathrm{gas}}}{\partial r} = \dfrac{\partial T_{\mathrm{cat}}}{\partial r} = 0 \\ \dfrac{\partial C_i}{\partial r} = 0 \end{cases} \tag{22}$$

$$(\mathrm{B}) \begin{cases} v_r = 0, \quad \dfrac{\partial v_z}{\partial z} = 0 \\ \dfrac{\partial T_{\mathrm{gas}}}{\partial z} = \dfrac{\partial T_{\mathrm{cat}}}{\partial z} = 0 \\ \dfrac{\partial C_i}{\partial z} = 0 \end{cases} \tag{23}$$

$$(\mathrm{C}) \begin{cases} v_r = v_z = 0, \quad \dfrac{\partial p}{\partial r} = 0 \\ \dfrac{\partial T_{\mathrm{gas}}}{\partial r} = \dfrac{\partial T_{\mathrm{cat}}}{\partial r} = 0 \\ \dfrac{\partial C_i}{\partial r} = 0 \end{cases} \tag{24}$$

$$(\mathrm{D}) \begin{cases} v_r = 0, \quad v_z = V_{in}, \quad p = p^{\mathrm{in}} \\ T_{v\mathrm{go}} = T_{v\mathrm{go}}^{\mathrm{in}}, \quad T_{\mathrm{cat}} = T_{\mathrm{cat}}^{\mathrm{in,c}} \\ C_{v\mathrm{go}} = C_{v\mathrm{go}}^{\mathrm{in}}, \quad C_i = 0 \ (i = 2 \text{ to } 6) \end{cases} \tag{25}$$

A mesh convergence criterion was defined to select a converged mesh for the computational domain of Figure 3, such that the Euclidean norm of the solution did not change in comparison with more refined meshes, by keeping the relative error of the Euclidean norm of the solution obtained with two meshes under comparison, below a pre-specified tolerance (10^{-3}). For the simulations presented, a converged 2-D mesh according to that criterion, in cylindrical coordinates, with 1500 volumes (10 in the r direction and 150 in the z direction) was found.

As is observed from the set of differential equations (Eqs. 1-3 and 15-17), the fluid flow problem (Eqs. 1-3) is not coupled with the thermal and reaction kinetic problem (Eqs. 15-17). This is explained by the fact that the physical properties, especially the mixture average density (ρ), are constant along the riser bed, allowing the incompressible formulation for the fluid flow. This simplification implies an error on the calculated velocity field. However, for industrial applications, the most important variables to be precisely determined are the mass flow rates of the lumps at the output section of the riser, which are not significantly affected by that simplification, as will be shown in the "Experimental Validation" section of this article. With this hypothesis, the set of differential equations can then be solved in two steps: i) for the velocities (fluid flow), and ii) for the concentrations (kinetic) and temperatures (energy).

Such simplification also results in a very stable numerical solution, with high convergence ratios, implying low computational time and processing capacity requirements. The entire simulation presented below (with a grid of 1500 volumes), in the most unfavorable situation, that is, when started without a previous approximated solution (restart data), converges in less than 15 min in an Intel Pentium III processor, with a 1 GHz clock and 512Mb of RAM memory. When a solution obtained previously for the same mesh is available, even from very different input data, the processing time can be reduced to less than 5 min.

Experimental Validation

The 6-lump reaction kinetic model is able to represent the major conversion characteristics of the gasoil into noble products. However, these kinetic models, especially those with just a few lumps and those that represent the feedstock by only 1 lump, in general cannot accurately predict different setups from those used in the model kinetic parameter estimation.

The hypotheses (simplifications) applied to the present mathematical formulation can also contribute to deviations between the available experimental data and the calculated results. When precise conversion profiles are necessary, the mathematical model (mainly the kinetic model) needs to be adjusted to a specific gasoil feedstock. This procedure was carried out in a previous study by one of the authors of this article,[16] by fitting constants to the mathematical formulation by the solution of the inverse problem of parameter estimation from the set of known experimental data.

The available experimental data were the 6 lumps mass fractions at the riser output and the reaction temperature. Such quantities are obtained numerically with the model from the lump molar concentrations as follows:

$$Y_i = \frac{\dot{m}_i}{\dot{m}_{\text{lumps}}} = C_i \frac{M_i}{\rho} \frac{\dot{m}_{\text{total}}}{\dot{m}_{\text{lumps}}} \quad (i = 1, N) \tag{26}$$

where $\dot{m}_{lumps} = \sum_{i=1}^{N} \dot{m}_i$ is the mass flow rate of lumps at the riser cross section.

Thus, it is possible to formulate the inverse problem up to a 7 elements vector of fitting constants. In fact, only 5 lumps mass fractions are needed, since the sixth lump mass fraction results from mass conservation. Therefore, the system of equations was set for 6 fitting constants. Five of these constants were assigned to multiply the pre-exponential constants of the gasoil reactions (second order reactions) of Eq. 10, for i = 1, and a sixth constant was assigned to multiply the gasoil (vgo) enthalpy reaction term in Eq. 16.

From the available experimental data set, for a particular feedstock type (from heavy oil), with 27 different operating conditions, 9 were selected to determine the fitting constants vector, by solving the inverse problem nine times. The other 18 known experimental operating conditions were then used to validate the adjusted model. The resulting average fitting constants vector found in the process was [7.98, 16.83, 42.42, 20.35, 16.19, 1.4]. The formulation of the inverse problem of parameter estimation and the fitting constants calculation details can be found in ref. [16].

Thus, the validation was performed by direct comparison of the numerical results of the model with the experimental data available from a multipurpose unit located at SIX/PETROBRAS (Brazilian Oil Company) in Sao Mateus do Sul, Parana/Brazil. A total of 18 different operating conditions were used for the model validation, as explained in the previous paragraphs. The input variables of the model are the physical properties, mass flow rates, and input temperatures of the catalyst, the steam, and the gasoil, variables that define the operating conditions of the unit. Table 1 shows the general operating conditions and the physical properties used for all runs. The specific operating conditions for the different runs are obtained by varying the catalyst-to-gasoil mass flow rate ratio (COR), the riser height (H), and the input temperature of the catalyst that comes from the regenerator ((T_{cat}^{in}).

Figure 4 shows three comparisons performed between the experimental data and the numerical results (H = 10, 14, and 18 m), and illustrates the influence of the height of the riser on product formation. A good agreement between the experimental data and the numerical results was obtained for all points. In all studied cases, the relative error between experimental and numerical values $(Y_{\text{exp}} - Y_{\text{num}})/Y_{\text{exp}}$ is less than 10% for gasoline and between 10-15% for LPG.

In Figure 5, which evaluates the influence of the input catalyst temperature, the numerical results and the experimental data are again in good agreement for three different catalyst input temperatures ((T_{cat}^{in} = 680, 700, and 720°C). Therefore, Figures 4 and 5, together with the other not shown for the sake of brevity 12 experimental validation runs, validate the mathematical model for future utilization in FCC riser control, design, and/or optimization.

Results and Discussion

After model validation, several simulations of an industrial FCC riser were performed in this study, considering operating conditions, and geometrical and physical parameters that are listed in Table 2. Normally, for industrial applications, the main goal of FCC riser simulations is to predict, for a particular set of operating conditions, the mass fraction of each component (gasoline, LPG, light cycle oil, and so on) at the riser output section, so that the set of input parameters may be changed, aiming to increase (or maximize) the conversion of a specific product. The procedure can be conducted with just a few model experimental validation tests in the unity. Then, with the experimentally validated model, precise numerical results are expected to be obtained for any other operating and geometric conditions, for the same type of feedstock. Therefore, many other tests could then be accurately simulated with a computer code, allowing fast, simple, and low cost adjustment (or maximization) of unit production, following market fluctuations.

Table 1. General Operating Conditions of the Experimental Multipurpose Unit

Geometry	
Total riser height, H	10, 14, and 18 m
Riser diameter, $2R$	0.0508 m
Feedstock	
Gasoil input mass flow rate, $\dot{m}_{vgo}^{in}$	170 kg h^{-1}
Gasoil and steam input temperature, $T_{vgo}^{in} = T_{st}^{in}$	220°C
Water vapor mass flow rate, $\dot{m}_{st}$	13 kg h^{-1}
Catalyst-to-gasoil mass flow rate ratio, COR	6.9–9.4
Input pressure, p^{in}	2.5 bar
Physical parameters	
Catalyst density, ρ_{cat}	1400 kg m^{-3}
Catalyst specific heat, Cp_{cat}	1.09 kJ kg^{-1} K^{-1}
Input temperature of catalyst that comes from the regenerator, T_{cat}^{in}	680–720°C
Gasoil (vapor) density, ρ_{vgo}	10 kg m^{-3}
Gasoil specific heat, Cp_{vgo}	2.5 kJ kg^{-1} K^{-1}
Steam (vapor) density, ρ_{st}	0.5 kg m^{-3}
Steam specific heat, Cp_{st}	2.0 kJ kg^{-1} K^{-1}
Gas phase viscosity, μ_{gas}	2.0×10^{-5} kg m^{-1} s^{-1}
Heat transfer coefficient between phases h_{gs}	1×10^{3} kW m^{-3} K^{-1}

The output mass fractions and their profiles along the height of the riser are shown in Figure 6. It is seen that the cracking reactions of the gasoil are more intense in the beginning of the riser (from 0 to 10 m, approximately), where the concentration gradients are higher, remaining practically unaltered at higher regions.

The average temperature profiles for the gas phase (gasoil and steam) and for the solid phase (catalyst) are shown in Figure 7. It is seen that the model is able to predict heat transfer between the two phases. At the bottom of the riser ($z = 0$ m), the catalyst is at 560°C and the gasoil at 320°C, approximately. As in the case of the lump profiles, the initial condition drastically changes in the beginning of the riser and both temperatures reach a common value, remaining in thermal equilibrium until the end of the riser. The point where the curves join is a direct function of the product between gas-particulate heat transfer coefficient and catalyst surface area to volume ratio ($h_{gs} = h\ A_{gs}$), whereas the final temperature at the end of the riser is a function of the cracking reactions and the mass balance between the phases.

The 2-D mass fractions fields for the gasoil, gasoline, and LPG lumps at each control volume are shown in Figure 8. The mass fractions for each control volume were calculated as the mass flow rate of the specific lump divided by the total mass flow rate in each volume element:

$$Y_i^k = \frac{\dot{m}_i^k}{\dot{m}_{lumps}^k} \tag{27}$$

where Y_i^k and $\dot{m}_i^k$ are the mass fraction and mass flow rate of component i inside the volume element k, respectively; and $\dot{m}_{lumps}^k = \Sigma_{i=1}^{N}\ \dot{m}_i^k$, with N equal to the number of lumps of the kinetic model, is the total lumps (including coke) mass flow rate in the volume element k. Therefore, the coke content of the catalyst for Eq. 14 is calculated as $C_c^k = \dot{m}_c^k/\dot{m}_{cat}^k$, where $\dot{m}_c^k = Y_c^k \dot{m}_{lumps}^k$.

Figure 8 shows the change in gasoil conversion, coke formation, and coke content of the catalyst along the riser height. It is seen that for each cross section of the riser, the velocity in the z direction varies from approximately two times the mean section velocity at the center of the riser to zero at the wall. This velocity profile induces a higher concentration of gasoil at

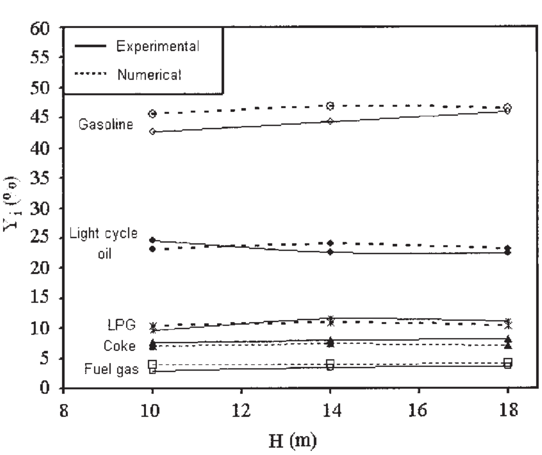

Figure 4. Lumps mass fractions as functions of the riser's height (T_{reac} = 550°C and T_{cat}^{in} = 680°C), and (H(m),COR) = (10,9.1;(14,9.4);(18,8.6).

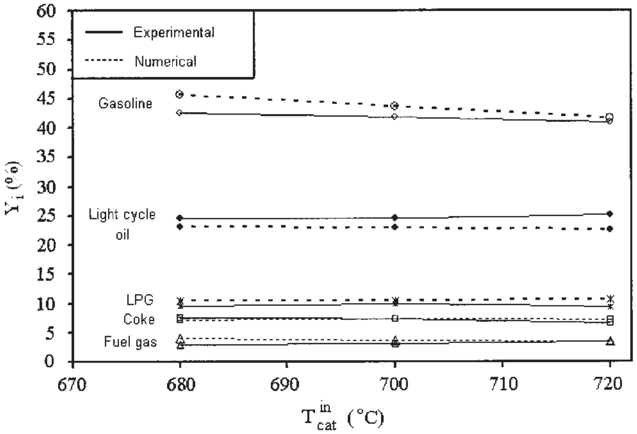

Figure 5. Lumps mass fractions as functions of the input catalyst temperature (T_{reac} = 550°C and H = 10 m), and (Γ_{cat}^{in} (°C), COR) = (680, 9.1); (700, 8.5); (720, 7.9).

Table 2. General Operating Characteristics of the Industrial FCC Riser Unit Considered in This Study[16]

Geometry	
Total riser height, H	32.8 m
Riser diameter, $2R$	0.6 m
Feedstock	
Gasoil input mass flow rate, $\dot{m}_{vgo}^{in}$	12744 kg h^{-1}
Gasoil and steam input temperature, $T_{vgo}^{in} = T_{st}^{in}$	320°C
Water vapor mass flow rate, $\dot{m}_{st}$	442.4 kg h^{-1}
Catalyst mass flow rate, $\dot{m}_{cat}$	62445.6 kg h^{-1}
Input pressure, p^{in}	2.5 bar
Physical parameters	
Input temperature of catalyst that comes from the regenerator, T_{cat}^{in}	567°C
Catalyst density, ρ_{cat}	1560 kg m^{-3}
Catalyst specific heat, Cp_{cat}	1.097 kJ kg^{-1} K^{-1}
Gasoil density, ρ_{vgo}	22 kg m^{-3}
Steam density, ρ_{st}	0.7 kg m^{-3}
Steam specific heat, Cp_{st}	2.0 kJ kg^{-1} K^{-1}
Gas phase viscosity, μ_{gas}	2.0×10^{-5} kg m^{-1} s^{-1}
Heat transfer coefficient between phases, h_{gs}	1×10^{3} kW m^{-3} K^{-1}

the center of the riser, whereas the concentration of gasoil decreases sharply near the wall, that is, nearly all gasoil that remains in that region is converted into products. It is important to bear in mind that the maximum conversion near the wall is not associated with the maximum mass flow rate; actually, quite the opposite, the maximum mass flow rate of gasoil occurs at the center of the riser.

The phenomenon of maximum conversion in the region near the riser wall is also experimentally observed in an industrial unity, although occurring for a different reason. In an actual industrial riser, the catalyst does not flow in only one direction in the riser. Near the wall, the shock of the solid particles with the wall makes the particulate lose part of its energy, and abruptly changes its velocity direction. This phenomenon increases the catalyst concentration near the wall and, depending on the operating conditions of the unity (mass flow rate ratio between the phases, mainly), it may cause the back slip of the catalyst on the wall and, therefore, the porosity near the wall tends to decrease. Thus, just like in the mathematical model presented here, in reality the gasoil concentration is higher in the center of the riser, and the conversion is higher in the region near the wall.

The radial concentration (mass fraction) profiles at four different cross sections of the riser are shown in Figure 9. These profiles are almost uniform along the radii of the riser, showing a small variation in the region near the wall, where the gasoil conversion is higher.

The 2-D temperature fields for the solid and gas phases are presented in Figure 10. The same phenomenon of higher concentration gradients in the beginning of the riser (Figure 8) is observed for the temperature fields. The average temperature profile shown in Figure 7 is confirmed with the two-dimensional temperature profiles. It should also be remembered that the temperature gradients are a result of two different phenomena: the heat transfer between the phases and the endothermic cracking reactions of the gasoil.

Conclusions

A simplified mathematical model for the numerical simulation of the fluid flow and the cracking reactions of the gasoil inside an FCC riser has been proposed, experimentally validated, and tested. The present formulation is theoretically simple and, numerically, results in low computational time to obtain solutions, if compared with more sophisticated tri-dimensional and two-phase models available in the literature. Nevertheless, it is still capable of determining, with good accuracy, the variables of interest to the oil refining industry: mass fractions of products at the output section and the temperature field in FCC riser units.

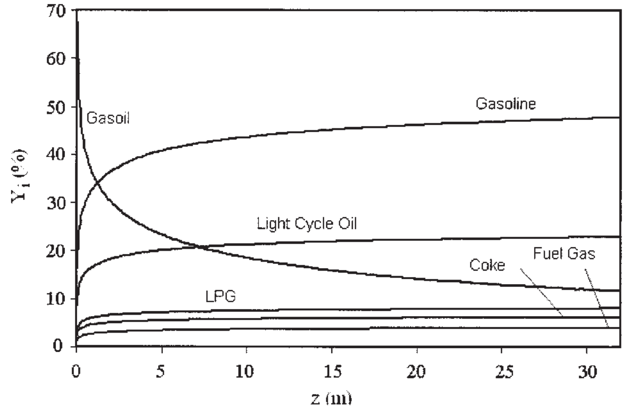

Figure 6. Mass fraction profiles along the industrial riser.

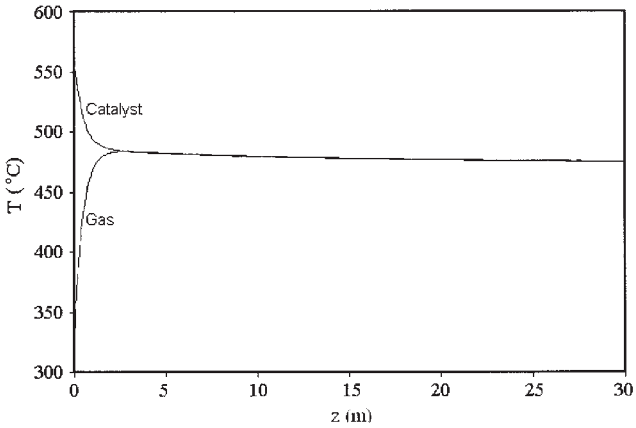

Figure 7. Average temperature profiles along the industrial riser.

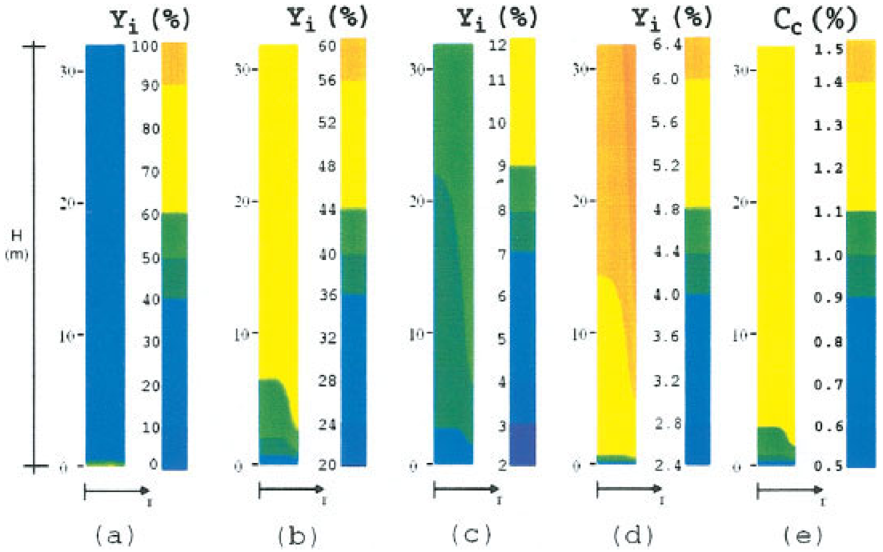

Figure 8. Two-dimensional mass fraction, Y_i, of gasoil (a), gasoline (b), LPG (c), coke (d), and coke content of the catalyst (e), C_c, along the industrial riser.

[Color figure can be viewed in the online issue, which is available at www.interscience.wiley.com.]

The formulation uses a 2-D fluid flow solution that is not coupled with the kinetic and energy solutions. This simplifies the numerical solution, increasing convergence rates and decreasing computational time. Even though the velocity field is not exact, it is better than that obtained by the plug flow approach and increases the ability of the numerical code to determine the lumps mass fractions at the riser output section.

The simulations presented in this article illustrate the applicability of the proposed model for the numerical simulation of an actual industrial FCC riser unity. The average mass fraction and temperature profiles along the height of the riser were presented and discussed. The 2-D fields of the mass fractions for the gasoil and the two main products of the FCC riser, gasoline and LPG, were graphically shown. The temperature profiles and 2-D temperature fields for both phases were also presented. The presented results demonstrate that the model can be used as a powerful and simple tool for design, control, and optimization of FCC units, combining accuracy with low computational time to obtain solutions when simulating actual FCC riser operation.

Acknowledgments

The authors acknowledge with gratitude the support of PRH-24/ANP/MCT, of project N° 1121/00 –CTPETRO/FINEP, and of SIX/PETROBRAS (Brazilian Oil Co.).

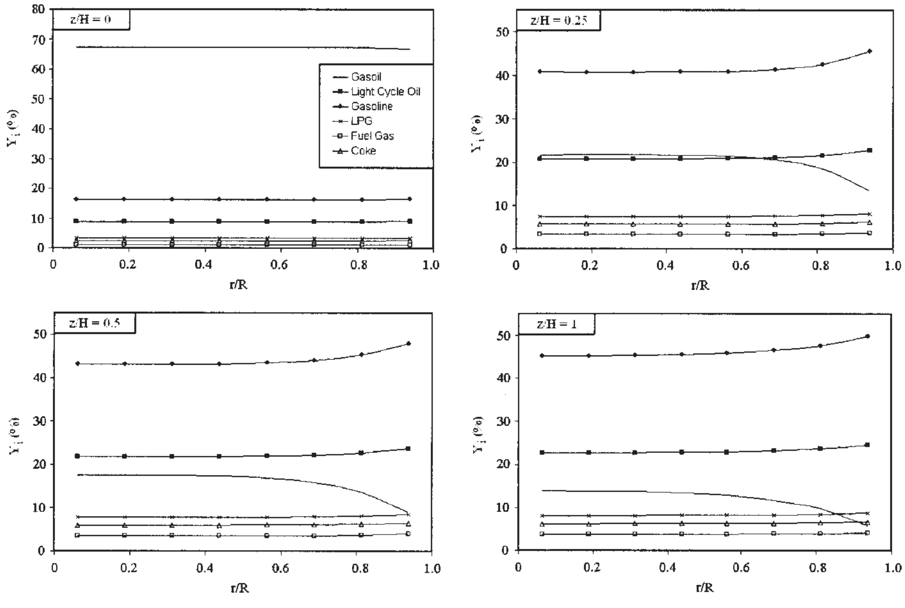

Figure 9. Radial mass fraction profiles for various cross sections along the industrial riser.

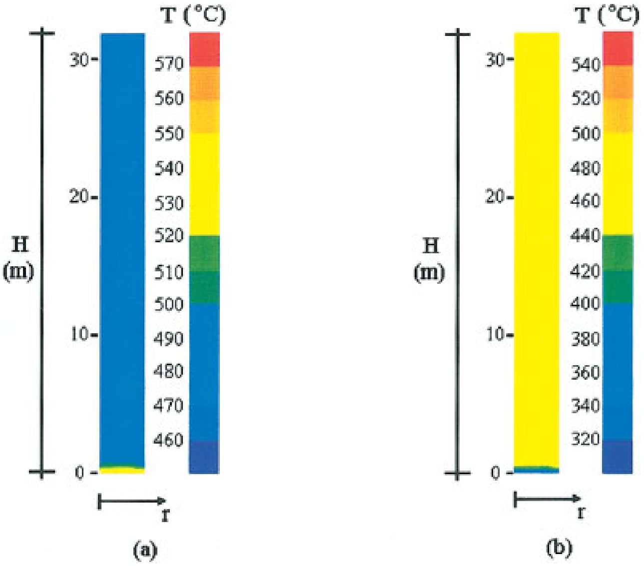

Figure 10. 2-D temperature profiles along the industrial riser: gaseous phase (a) and solid phase (b).

[Color figure can be viewed in the online issue, which is available at www.interscience.wiley.com.]

Notation

A = riser cross sectional area (m^2)
A_{gs} = specific surface area of the catalyst based on the unit reactor volume ($m^2\ m^{-3}$)
C = lump concentration (kmol m^{-3})
C_c = coke content of the catalyst ($kg_c\ kg_{cat}^{-1}$)
Cp = specific heat (kJ $kg^{-1}\ K^{-1}$)
COR = catalyst-to-gasoil mass flow rate ratio, $\dot{m}_{cat}\ (\dot{m}_{vgo}^{in})^{-1}$
Δh = reaction specific enthalpy (kJ kg^{-1})
E = activation energy (kJ $kmol^{-1}$)
h = gas-solid heat transfer coefficient (kW $m^{-2}\ K^{-1}$)
h_{fg} = specific evaporation enthalpy (kJ kg^{-1})
h_{gs} = product between gas-solid heat transfer coefficient and specific surface area of the catalyst based on the unit reactor volume, $h_{gs}A_{gs}$ (kW $m^{-3}\ K^{-1}$)
H = total riser height (m)
K = pre-exponential kinetic constant ($m^3\ kg_{cat}^{-1}$ s or $m^6\ kmol^{-1}\ kg_{cat}^{-1}\ s^{-1}$)
K^r = kinetic reaction constant ($m^3\ kg_{cat}^{-1}\ s^{-1}$ or $m^6\ kmol^{-1}\ kg_{cat}^{-1}\ s^{-1}$)
$\dot{m}$ = mass flow rate (kg s^{-1})
M = molecular weight (kg $kmol^{-1}$)
n = reaction order
N = number of lumps
p = pressure (Pa)
R = riser radius (m)
$\bar{R}$ = universal gas constant (kJ $kmol^{-1}\ K^{-1}$)
r, z = cylindrical coordinates (m)
t = time (s)
T = temperature (K)
v_r, v_z = fluid velocities (m s^{-1})
V_{in} = riser fluid flow input velocity (m s^{-1})
$\forall$ = volumetric flow rate ($m^3\ s^{-1}$)
Y = mass fraction

Greek letters

ε = bed porosity
μ = viscosity (kg $m^{-1}\ s^{-1}$)
ν = kinematic viscosity ($m^2\ s^{-1}$)
ρ = density (kg m^{-3})
ρ = average mixture density (kg m^{-3}), Eq. 4
ϕ = deactivation function
φ = volume fraction
Ω = volumetric rate of creation or consumption of species in the reaction (kmol $m^{-3}\ s^{-1}$)

Subscripts

ad = adsorption
c = coke
cat = catalyst
exp = experimental
gas = gaseous phase
gs = gas-solid
i, j = indexes for the lumps
$lumps$ = lumps
num = numerical
$reac$ = reaction
st = water steam
$total$ = total
vgo = gasoil
w = water

Superscripts

c = corrected
i, j = indexes for the lumps
in = input
k = grid volume element index
r = reaction

Literature Cited

1. Theologos KN, Markatos NC. Advanced modeling of fluid catalytic cracking riser-type reactors. *AIChE J.* 1993;39(6):1007-1017.
2. Gao JS, Xu CM, Lin SX, Yang GH, Guo YC. Simulations of gas-liquid-solid 3-phase flow and reaction in FCC riser reactors. *AIChE J.* 2001;47(3):677-692.
3. Han IS, Chung CB. Dynamic modeling and simulation of a fluidized catalytic cracking process. Part I: Process modeling. *Chem Eng Sci.* 2001;56(5):1951-1971.
4. Martignoni WP. Modelling and simulation of FCC riser reactors: a heterogeneous approach. Ph.D. Thesis, University of Western Ontario, Ontario, Canada, 1998.
5. Ali H, Rohani S. Dynamic modeling and simulation of a riser-type fluid catalytic cracking unit. *Chem Eng Technol.* 1997;20(2):118-130.
6. Martignoni W, de Lasa HI. Heterogeneous reaction model for FCC riser units. *Chem Eng Sci.* 2001;56(2):605-612.
7. Patience GS, Chaouki J, Berruti F, Wong R. Scaling considerations for circulating fluidized bed risers. *Powder Technol.* 1992;72(1):31-37.
8. Derouin C, Nevicato D, Forissier M, Wild G, Bernard JR. Hydrodynamics of riser units and their impact on FCC operation. *Industrial Eng Chem Research.* 1997;36(11):4504-4515.
9. Berry TA, McKeen TR, Pugsley TS, Dalai AK. Two-dimensional reaction engineering model of the riser section of a fluid catalytic cracking unit. *Industrial Eng Chem Research.* 2004;43(18):5571-5581.
10. Chang SL, Zhou CQ. Simulation of FCC riser flow with multiphase heat transfer and cracking reactions. *Computational Mechanics.* 2003;31(6):519-532.
11. Ali H, Rohani S, Corriou JP. Modelling and control of a riser type fluid catalytic cracking (FCC) unit. *Chem Eng Research Design.* 1997;75(A4):401-412.
12. Cerqueira HS, Biscaia EC Jr., Aguiar EFS. Mathematical modeling of deactivation by coke formation in the cracking of gasoil. *Studies in Surface Sci Catalysis.* 1997a;111:303-310.
13. Cerqueira HS, Biscaia EC, Sousa-Aguiar EF. Mathematical modeling and simulation of catalytic cracking of gasoil in a fixed bed: coke formation. *Applied Catalysis A General.* 1997b;164(1-2):35-45.
14. Ancheyta J, Lopez-Isunza F, Aguilar-Rodriguez E. 5-lump kinetic model for gasoil catalytic cracking. *Applied Catalysis A General.* 1999;177(2):227-235.
15. Han IS, Riggs JB, Chung CB. Modeling and optimization of a fluid-

ized catalytic cracking process under full and partial combustion modes. *Chem Eng Proc.* 2004;43(8):1063-1084.

16. Souza JA. Numerical simulation and thermodynamic optimization of fluidized catalytic cracking risers for maximizing fuel production. Doctoral Thesis, Federal University of Parana, Curitiba, PR, Brazil (*in Portuguese*), 2004.
17. Petrobras Six. List of kinetic parameters and Arrhenius constants for the 6-lump model. Internal report (*in Portuguese*). São Mateus do Sul-PR-Brazil; 2001.
18. Pitault I, Nevicato D, Forissier M, Bernard JR. Kinetic model based on a molecular description for catalytic cracking of vacuum gasoil. *Chem Eng Sci.* 1994;49(24A):4249-4262.
19. Jacob SM, Gross B, Voltz SE, Weekman Jr. VW. Lumping and reaction scheme for catalytic cracking. *AIChE J.* 1976;22(4):701-713.
20. Miller A, Gidaspow D. Dense, vertical gas-solid flow in a pipe. *AIChE J.* 1992;38(11):1801-1815.

Manuscript received Oct. 20, 2005, and revision received Jan. 7, 2006.